

Article

# The Effect of Niobium on the Changing Behavior of Non-Metallic Inclusions in Solid Alloys Deoxidized with Mn and Si during Heat Treatment at 1473 K

Chengsong Liu <sup>1</sup>, Xiaoqin Liu <sup>1,\*</sup>, Shufeng Yang <sup>2</sup>, Jingshe Li <sup>2</sup>, Hongwei Ni <sup>1</sup> and Fei Ye <sup>1</sup>

<sup>1</sup> The State Key Laboratory of Refractories and Metallurgy, Wuhan University of Science and Technology, Wuhan 430081, China; liuchengsong@wust.edu.cn (C.L.); nihongwei@wust.edu.cn (H.N.); yefeishangnan@163.com (F.Y.)

<sup>2</sup> School of Metallurgical and Ecological Engineering, University of Science and Technology Beijing, Beijing 100083, China; yangshufeng@ustb.edu.cn (S.Y.); lijingshe@ustb.edu.cn (J.L.)

\* Correspondence: liuxiaoqin@wust.edu.cn; Tel.: +86-27-6886-2811

Received: 4 April 2017; Accepted: 13 June 2017; Published: 16 June 2017

**Abstract:** To clarify the effect of niobium (Nb) on the changing behavior of oxide inclusions in alloys containing different concentrations of Mn, Si, and Nb, heat treatment experiments at 1473 K were conducted and changes in the morphology, size, quantity, and composition of these inclusions were investigated. The stability of the oxide inclusions in both molten and solid Fe-Mn-Si-Nb alloys was also estimated by thermodynamic calculation using available data. Results showed that the change in the composition of the oxide inclusions owing to heat treatment depended on the concentrations of Nb and Si in the alloy. MnO-SiO<sub>2</sub>-type oxide inclusions gradually transformed into MnO-Nb<sub>2</sub>O<sub>5</sub>-type or MnO-SiO<sub>2</sub>- & MnO-Nb<sub>2</sub>O<sub>5</sub>-type inclusions in low-Si and high-Nb alloys after heating for 60 min. However, the shape of the inclusions did not change clearly. It was indicated that, during the heat treatment at 1473 K, an interface chemical reaction between the Fe-Mn-Si-Nb alloys and the MnO-SiO<sub>2</sub>-type oxide inclusions occurred according to the experimental and calculation results.

**Keywords:** niobium; non-metallic inclusion; heat treatment; interfacial reaction; modification

## 1. Introduction

By oxide metallurgy technology, fine and dispersed non-metallic inclusions in steel could not only distribute around austenite boundaries to restrain grain growth but also act as heterogeneous nucleus to promote acicular ferrite, which are able to greatly improve the mechanical properties of steel [1–4]. Heat treatment is a new approach to precisely controlling and optimizing the physicochemical characteristics of non-metallic inclusions in steel and greatly expanding the application of oxide metallurgy technology in steel production, which is attracting more and more attention. Shibata et al. [5] reported that, in the Fe-Cr alloy containing 10 mass % Cr, MnO-SiO<sub>2</sub>-type inclusions transformed into MnO-Cr<sub>2</sub>O<sub>3</sub>-type inclusions with a low Si content (<0.1 mass %) after heat treatment, while at high Si content (>0.3 mass %), the MnO-SiO<sub>2</sub>-type inclusion was stable. Choi et al. [6] hypothesized that, in an as-cast Fe-0.028 mass % Ti alloy, Ti-O inclusions with a small amount of Fe gradually changed to Ti-Fe-O after heating at 1473 K for 180 min. The fraction of fine and coarse inclusions increased and decreased, respectively. Shao et al. [7] confirmed that shape variation of slender MnS was greatly influenced by the heating rate. As heating rate rose from 0.5 to 2 K/s, the amount of split MnS decreased; while the heating rate exceeded 6 K/s, the slender MnS remained unchanged. Liu et al. [8] studied solid-state reactions between an Fe-Al-Ca alloy and an Al<sub>2</sub>O<sub>3</sub>-CaO-FeO oxide during heat treatment at 1473 K and found that some Al<sub>2</sub>O<sub>3</sub> particles and CaO·Al<sub>2</sub>O<sub>3</sub> branch inclusions precipitated as reaction products in the alloy near the alloy-oxide

interface, which caused the Al content in the alloy to decrease. They also [9] investigated an interfacial reaction mechanism between CaO-SiO<sub>2</sub>-Al<sub>2</sub>O<sub>3</sub>-MgO-MnO oxides and a Fe-Mn-Si alloy during heating. It was proved that the overall MnO and SiO<sub>2</sub> content of the oxide decreased and increased, respectively, after the “solid–liquid” reaction between the oxide and alloy at 1473 K.

As an important alloying element with a broad application prospect, the niobium (Nb) added into the alloy is beneficial for the precipitation of inclusion particles such as Nb(C, N), which prevents the growth of austenite grain by the pinning effect at the grain boundaries during heat treatment [10,11]. By combining with solute Nb in alloy, Nb(C, N) particles can also inhibit the recrystallization of deformed austenite through the drag effect and promote fine acicular-ferrite. Moreover, Nb contributes to the dispersive distribution of inclusions and a flexible adjustment of the toughness of the alloy in a broad range by controlling the induced precipitation and cooling rate. Therefore, Nb in the alloy can not only enhance the strength of the alloy but also improve the toughness, the high temperature oxidation resistance, and the corrosion resistance of the alloy and reduce the brittle transition temperature of the alloy to obtain a better welding and forming performance. Nevertheless, other than the precipitation of particles such as Nb(C, N), heat treatment also results in changes in composition, morphology, size, and the physicochemical characteristics of other inclusions with the influence of elemental Nb, which directly affects the quality and mechanical properties of the alloy.

In the present study, experiments were designed to reveal the effect of Nb on the changing behavior of non-metallic inclusions in the Fe-Mn-Si-Nb alloy including morphology, types, compositions, and quantities during heat treatment at 1473 K. The stability of the oxide inclusions in both molten and solid Fe-Mn-Si-Nb alloys was also discussed in light of thermodynamic calculations.

## 2. Experimental Methods

### 2.1. Materials

Initial compositions of the alloys with different concentrations of Mn, Si, and Nb are summarized in Table 1. A 6 kg Fe-Mn-Si ingot was prepared by melting electrolytic iron with ferromanganese and silicon powder in an arc melting furnace. Then, 200 g of the premelted Fe-Mn-Si alloy was taken from the position between the center and the edge of the circular cross section in the middle part of the ingot and then re-melted with the addition of high-grade ferroniobium in an MgO crucible (outer diameter 48 mm, inner diameter 38 mm, height 115 mm) at 1873 K for 15 min, under an air atmosphere in an electric resistance pipe furnace. After that, the crucible was taken out from the pipe and quenched by immersing the crucible into water. Due to the high cooling rate and small size of the alloy specimen, concentrations of Mn, Si, and Nb were firstly confirmed to be homogeneous by using an Electron Probe Microscopic Analyzer (EPMA) (JEOL, Tokyo, Japan) whose primary importance is the ability to acquire precise, quantitative elemental analyses at very small “spot” sizes (as little as 1–2 microns), primarily by wavelength-dispersive spectroscopy (WDS), and then measured and verified by Inductively Coupled Plasma Optical Emission Spectrometer (ICP-OES) (Thermo Fisher Scientific, Waltham, MA, USA).

**Table 1.** Initial compositions of the alloy deoxidized with Mn and Si for heat treatment at 1473 K.

Sample	Mass %					
	Fe	Mn	Si	Nb		
1	High Si	High Nb	97.57	0.63	1.09	0.61
2	Medium Si	High Nb	98.21	0.67	0.37	0.65
3	Low Si	High Nb	98.60	0.61	0.025	0.67
4	High Si	Medium Nb	98.07	0.68	1.12	0.13
5	Medium Si	Medium Nb	98.72	0.72	0.41	0.15
6	Low Si	Medium Nb	99.11	0.65	0.028	0.16
7	High Si	Low Nb	98.13	0.67	1.06	0.04
8	Medium Si	Low Nb	98.84	0.72	0.39	0.05
9	Low Si	Low Nb	99.20	0.73	0.023	0.05

## 2.2. Heat Treatment

The quenched alloy specimens were machined into cylindrical pieces ( $\phi$  10 mm  $\times$  20 mm) and hanged in the reaction pipe of an electric furnace by Mo wire. Then, specimens were heated at 1473 K for 30 min and 60 min, and the atmosphere was replaced by high purity Ar gas (99.9 mass %, flow rate: about 300 cm<sup>3</sup>/min). After above heat treatment, the specimens were immediately taken out of the reaction pipe and quenched by immersion into water. The temperature curve of heat treatment experiment is given in Figure 1. Schematic diagram of the furnace equipped with specimen quenching under a controlled Ar gas atmosphere for heat treatment is shown in Figure 2.

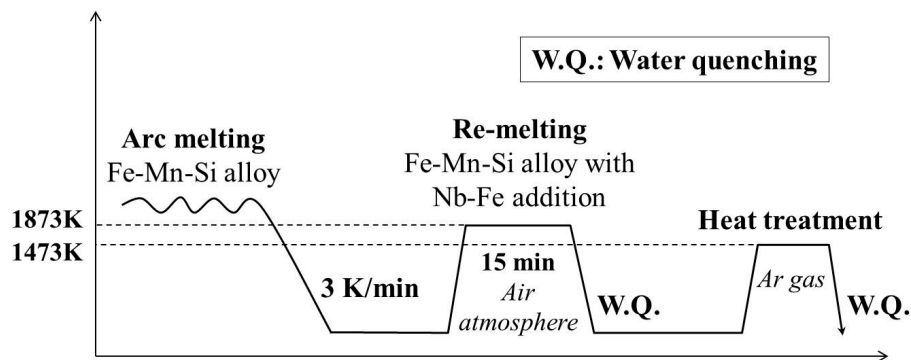


**Figure 1.** Temperature curve of melting and heat treatment experiments for Fe-Mn-Si-Nb specimens.

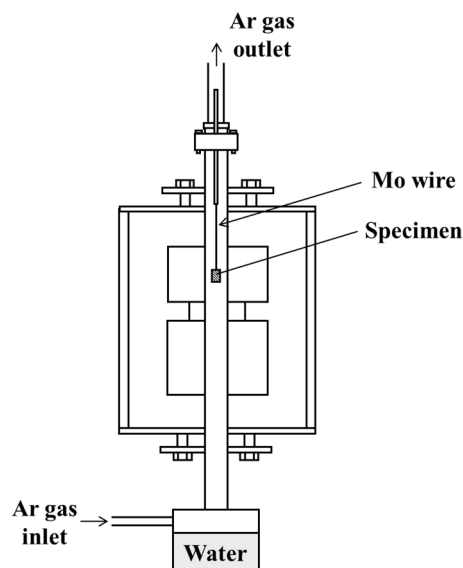


**Figure 2.** Schematic diagram of the furnace equipped with specimen quenching under controlled Ar gas atmosphere for heat treatment at 1473 K.

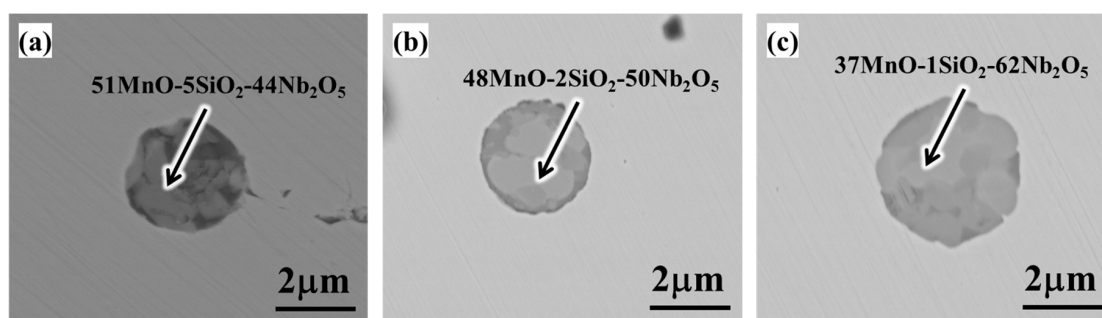
## 2.3. EPMA Analysis

As cast and heated specimens were embedded in the polyester resin, and the cross section of each specimen was ground with SiC sandpapers and polished with diamond polishing paste to prepare metallographic samples. Characteristics including morphology, types, quantities, and compositions of over 50 inclusions in each metallographic sample before and after heat treatment for 30 min and 60 min were observed and analyzed by an Electron Probe Microscopic Analyzer (EPMA), and the compositions of Fe, Mn, Si, and Nb were determined.

### 3. Results

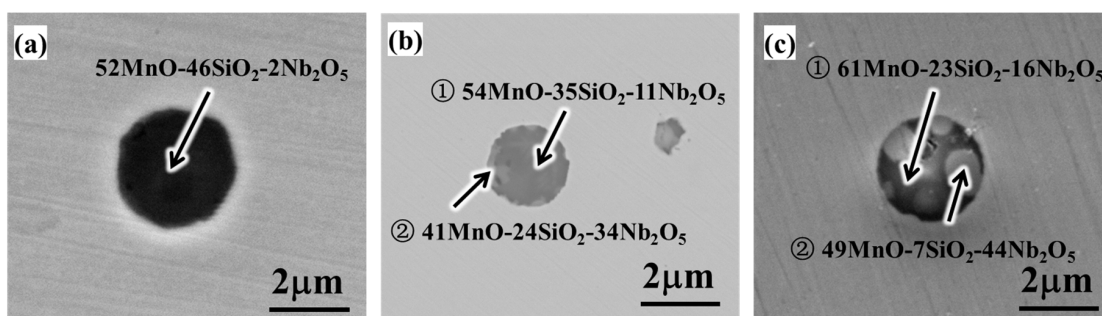
#### 3.1. Influence of Heat Treatment at 1473 K on the Morphology and Compositions of Oxide Inclusions

Figure 3 shows the morphology and compositions of typical oxide inclusions in Alloy Sample 2 (Mn: 0.67 mass %, Si: 0.37 mass %, Nb: 0.65 mass %). In an as-cast sample, nearly spherically shaped inclusions were observed. Their typical chemical composition, measured by using the EPMA, was 51 mol % MnO-5 mol % SiO<sub>2</sub>-44 mol % Nb<sub>2</sub>O<sub>5</sub>. After the heat treatment at 1473 K for 30 and 60 min, the shape of inclusions did not clearly change. The chemical compositions of these inclusions were 48 mol % MnO-2 mol % SiO<sub>2</sub>-50 mol % Nb<sub>2</sub>O<sub>5</sub> and 37 mol % MnO-1 mol % SiO<sub>2</sub>-62 mol % Nb<sub>2</sub>O<sub>5</sub>, respectively. This meant that only MnO-Nb<sub>2</sub>O<sub>5</sub>-type inclusions were observed in the case where Nb content in the alloy sample was higher than 0.6 mass %.



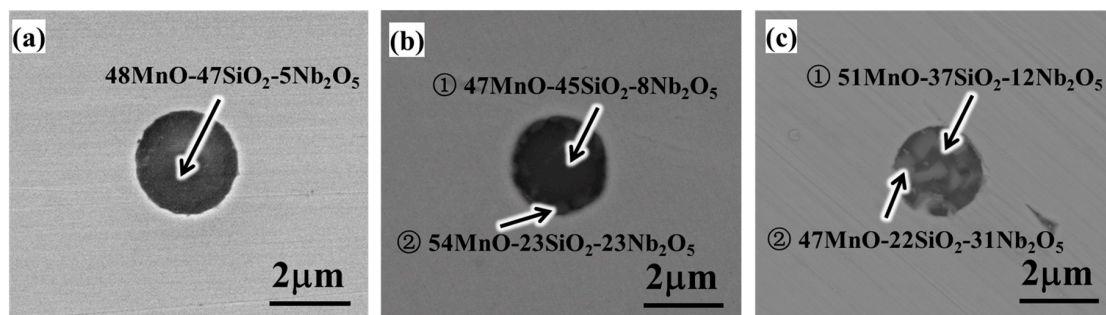
**Figure 3.** Morphology and compositions of typical oxide inclusions in Alloy Sample 2: (a) as cast; (b) heat treatment for 30 min; (c) heat treatment for 60 min.

Figure 4 shows the morphology and compositions of typical oxide inclusions in Alloy Sample 4 (Mn: 0.68 mass %, Si: 1.12 mass %, Nb: 0.13 mass %). The spherically shaped MnO-SiO<sub>2</sub>-type inclusion was also found in an as-cast sample. Its typical chemical composition was 52 mol % MnO-46 mol % SiO<sub>2</sub>-2 mol % Nb<sub>2</sub>O<sub>5</sub>. After heating at 1473 K for 30 min, although the shape of inclusions still did not clearly change, many inclusions had two phases in an inclusion, as Figure 4b shows the typical morphology of inclusions in Alloy Sample 4. One is MnO-SiO<sub>2</sub>-type inclusion containing approximately 11 mol % Nb<sub>2</sub>O<sub>5</sub>. The other is Mn-Si-Nb inclusion, whose average composition is 41 mol % MnO-24 mol % SiO<sub>2</sub>-34 mol % Nb<sub>2</sub>O<sub>5</sub>. As the heating time increased to 60 min, the Nb<sub>2</sub>O<sub>5</sub> content of both phases in an inclusion increased, as shown in Figure 4c. Their typical chemical compositions were 61 mol % MnO-23 mol % SiO<sub>2</sub>-16 mol % Nb<sub>2</sub>O<sub>5</sub> and 49 mol % MnO-7 mol % SiO<sub>2</sub>-44 mol % Nb<sub>2</sub>O<sub>5</sub>, respectively. This phenomenon indicated that the chemical composition of the oxide inclusions changed by heat treatment in the cases of medium Nb content and high Si content.



**Figure 4.** Morphology and compositions of typical oxide inclusions in Alloy Sample 4: (a) as cast; (b) heat treatment for 30 min; (c) heat treatment for 60 min.

The morphology and compositions of typical oxide inclusions observed in Alloy Sample 8 (Mn: 0.72 mass %, Si: 0.39 mass %, Nb: 0.05 mass %) were shown in Figure 5. The main shape and composition of inclusions found in the as-cast sample and their changing behavior with heating were similar to those observed in the case of Alloy Sample 4. Many observed inclusions in Alloy Sample 8 after heating also had two phases as shown in Figure 5b,c, and the Nb<sub>2</sub>O<sub>5</sub> content of both phases in an inclusion appears to be relatively lower, dependent on the concentrations of Nb and Si in the alloy. After heat treatment at 1473 K for 30 min, typical chemical compositions of the two phases in an inclusion were 47 mol % MnO-45 mol % SiO<sub>2</sub>-8 mol % Nb<sub>2</sub>O<sub>5</sub> and 54 mol % MnO-23 mol % SiO<sub>2</sub>-23 mol % Nb<sub>2</sub>O<sub>5</sub>, respectively. After heat treatment for 60 min, the concentrations of Nb<sub>2</sub>O<sub>5</sub> in the two phases in an inclusion increased to 12 mol % and 31 mol %, while SiO<sub>2</sub> concentrations decreased to 37 mol % and 22 mol %, respectively.



**Figure 5.** Morphology and compositions of typical oxide inclusions in Alloy Sample 8: (a) as cast; (b) heat treatment for 30 min; (c) heat treatment for 60 min.

### 3.2. Influence of Nb, Si and Mn Contents of the Alloy on Change in Type and Quantity of Oxide Inclusions

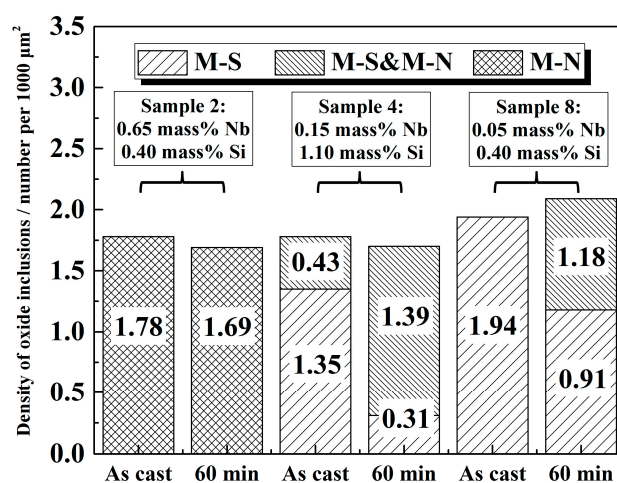
The dependence of chemical compositions of stable oxide inclusions on the concentrations of Mn, Si, and Nb in different alloy samples before and after heating at 1473 K for 60 min is shown in Table 2. In this table, alloy samples containing MnO-SiO<sub>2</sub>-type and MnO-Nb<sub>2</sub>O<sub>5</sub>-type inclusions are denoted by white circles and black circles, respectively. Moreover, the alloy sample containing both types of inclusions is denoted by crosses. Only MnO-Nb<sub>2</sub>O<sub>5</sub>-type inclusions formed in Alloy Samples 1–3 containing about 0.65 mass % Nb before and after heating at 1473 K for 60 min, which was very stable although Si content varied from 0.025 mass % to 1.10 mass %. As for the chemical compositions of oxide inclusions in Alloy Samples 4–6 containing about 0.15 mass % Nb, with the decrease in Si content in the as-cast sample, MnO-SiO<sub>2</sub>-type inclusions gradually disappeared and MnO-SiO<sub>2</sub>- & MnO-Nb<sub>2</sub>O<sub>5</sub>-type and MnO-Nb<sub>2</sub>O<sub>5</sub>-type inclusions formed. After the heat treatment at 1473 K, original MnO-SiO<sub>2</sub>-type and MnO-SiO<sub>2</sub>- & MnO-Nb<sub>2</sub>O<sub>5</sub>-type inclusions in the as-cast samples changed to MnO-SiO<sub>2</sub>- & MnO-Nb<sub>2</sub>O<sub>5</sub>-type and MnO-Nb<sub>2</sub>O<sub>5</sub>-type inclusions, respectively. When the Nb content decreased to 0.05 mass % in Alloy Samples 7–9, inclusions in the as-cast samples were mainly MnO-SiO<sub>2</sub>-type or MnO-SiO<sub>2</sub>- & MnO-Nb<sub>2</sub>O<sub>5</sub>-type before heat treatment depending on the concentration of Si in the alloy. After the heat treatment, some of the original MnO-SiO<sub>2</sub>-type inclusions transformed into two-phase MnO-SiO<sub>2</sub>- & MnO-Nb<sub>2</sub>O<sub>5</sub>-type inclusions, while some of the original two-phase MnO-SiO<sub>2</sub>- & MnO-Nb<sub>2</sub>O<sub>5</sub>-type inclusions transformed into MnO-Nb<sub>2</sub>O<sub>5</sub>-type inclusions, although the transformation was incomplete. The results strongly indicate that the relatively high Si content and low Nb content retard the conversion from a MnO-SiO<sub>2</sub>-type to a MnO-Nb<sub>2</sub>O<sub>5</sub>-type inclusion. This retardation occurs as long as non-equilibrium conditions persist between the alloy and the MnO-SiO<sub>2</sub>-type oxide inclusion.

Figure 6 shows the statistical analysis of the density of oxide inclusions changing from MnO-SiO<sub>2</sub>-type to MnO-SiO<sub>2</sub>- & MnO-Nb<sub>2</sub>O<sub>5</sub>-type and MnO-Nb<sub>2</sub>O<sub>5</sub>-type in Alloy Samples 2, 4, and 8. At least 120 random inclusions in each sample including MnO-SiO<sub>2</sub>-type, MnO-SiO<sub>2</sub>- & MnO-Nb<sub>2</sub>O<sub>5</sub>-type and MnO-Nb<sub>2</sub>O<sub>5</sub>-type were measured and analyzed by EPMA.

**Table 2.** Dependence of chemical compositions of stable oxide inclusions on the concentrations of Mn, Si, and Nb in different alloy samples before and after heating at 1473 K for 60 min.

Sample	No.	Heating Time	As Cast	60 min
Fe-0.65 mass % Nb	1	High Si (1.10 mass %)	●	●
	2	Medium Si (0.40 mass %)	●	●
	3	Low Si (0.025 mass %)	●	●
Fe-0.15 mass % Nb	4	High Si (1.10 mass %)	○×	×
	5	Medium Si (0.40 mass %)	×	×●
	6	Low Si (0.025 mass %)	●	●
Fe-0.05 mass % Nb	7	High Si (1.10 mass %)	○	○×
	8	Medium Si (0.40 mass %)	○	○×
	9	Low Si (0.025 mass %)	×	×●

Note: ○—MnO-SiO<sub>2</sub>-type; ×—MnO-SiO<sub>2</sub>- & MnO-Nb<sub>2</sub>O<sub>5</sub>-type; ●—MnO-Nb<sub>2</sub>O<sub>5</sub>-type.

**Figure 6.** Statistical analysis of the quantity of oxide inclusions changing from MnO-SiO<sub>2</sub>-type to MnO-SiO<sub>2</sub>- & MnO-Nb<sub>2</sub>O<sub>5</sub>-type and MnO-Nb<sub>2</sub>O<sub>5</sub>-type in Alloy Samples 2, 4, and 8.

It is clear that all inclusions observed in Alloy Sample 2 were MnO-Nb<sub>2</sub>O<sub>5</sub>-type before and after the heating at 1473 K. For Alloy Sample 4, there were 1.35 MnO-SiO<sub>2</sub>-type inclusions and 0.43 MnO-SiO<sub>2</sub>- & MnO-Nb<sub>2</sub>O<sub>5</sub>-type inclusions within the area of 1000 μm<sup>2</sup> in the as-cast sample, while after the heat treatment, the density of MnO-SiO<sub>2</sub>-type inclusions and MnO-SiO<sub>2</sub>- & MnO-Nb<sub>2</sub>O<sub>5</sub>-type inclusions increased to 1.39 and decreased to 0.31 in the area of 1000 μm<sup>2</sup>, respectively. In Alloy Sample 8, the original density of MnO-SiO<sub>2</sub>-type inclusions in the as cast was 1.94 per 1000 μm<sup>2</sup>, and then about half of them changed to MnO-SiO<sub>2</sub>- & MnO-Nb<sub>2</sub>O<sub>5</sub>-type inclusions after the heating at 1473 K for 60 min. By comparing the statistical results of the density of oxide inclusions in Alloy Samples 2, 4, and 8 before and after heat treatment, it was proved that there was no new formation of MnO-Nb<sub>2</sub>O<sub>5</sub>-type and MnO-SiO<sub>2</sub>- & MnO-Nb<sub>2</sub>O<sub>5</sub>-type inclusions during heating besides the transformation from the MnO-SiO<sub>2</sub>-type inclusions. It was also clearly found that the relatively high Nb content and low Si content promoted the transformation from MnO-SiO<sub>2</sub>-type inclusion to two-phase MnO-SiO<sub>2</sub>- & MnO-Nb<sub>2</sub>O<sub>5</sub>-type and MnO-Nb<sub>2</sub>O<sub>5</sub>-type inclusions.

## 4. Discussion

### 4.1. Mechanism of the Interface Reaction between the Alloy and M-S-Type Inclusion

Elemental Mn, Si, and Nb in the alloy could react with dissolved oxygen to form complex oxide inclusions, due to exposure to air atmosphere when preparing the alloy samples. It is generally known

that both manganese and niobium are transition metals and could take several different valences in oxides including  $\text{Mn}^{2+}$ ,  $\text{Mn}^{3+}$ ,  $\text{Mn}^{4+}$ ,  $\text{Nb}^{2+}$ ,  $\text{Nb}^{3+}$ ,  $\text{Nb}^{4+}$ , and  $\text{Nb}^{5+}$ . Under the oxygen partial pressure of steelmaking,  $\text{Mn}^{2+}$  is dominant among other different valence states in its oxide form of  $\text{MnO}$  [12], and Nb seems to be stable as  $\text{Nb}^{5+}$  in solid oxide under an oxidizing atmosphere (i.e.,  $\text{Nb}_2\text{O}_5$ ) [13]. In addition, compared with  $\text{SiO}$ ,  $\text{SiO}_2$  is much more stable during the oxidation of silicon in the alloy. Therefore, during the re-melting of Fe-Mn-Si-Nb alloy at 1873 K under air atmosphere, stable simple oxides of Mn, Si, and Nb were  $\text{MnO}$ ,  $\text{SiO}_2$ , and  $\text{Nb}_2\text{O}_5$ , respectively. Moreover, according to the stable components in the ternary system  $\text{Nb}_2\text{O}_5$ - $\text{MnO}$ - $\text{SiO}_2$  [14],  $\text{MnO}$ - $\text{SiO}_2$ -type,  $\text{MnO}$ - $\text{Nb}_2\text{O}_5$ -type, and  $\text{MnO}$ - $\text{SiO}_2$ - &  $\text{MnO}$ - $\text{Nb}_2\text{O}_5$ -type oxides could be acquired, except for  $\text{SiO}_2$ - $\text{Nb}_2\text{O}_5$ -type oxide.

In this study, influenced by the chemical compositions of the alloys, the changing behavior of inclusion from original  $\text{MnO}$ - $\text{SiO}_2$ -type to  $\text{MnO}$ - $\text{SiO}_2$ - &  $\text{MnO}$ - $\text{Nb}_2\text{O}_5$ -type and  $\text{MnO}$ - $\text{Nb}_2\text{O}_5$ -type was confirmed after heating at 1473 K for 60 min. It was indicated that there are interfacial reactions that occur between the alloy and the  $\text{MnO}$ - $\text{SiO}_2$ -type inclusions in some alloy samples. Inclusions equilibrated with a molten alloy at 1873 K are no longer stable in a solid-state alloy. A schematic of the interface reaction mechanism is shown in Figure 7. As the heat treatment time increased, the Nb in the alloy gradually diffused and reacted with the inclusions, thereby resulting in the formation of  $\text{MnO}$ - $\text{SiO}_2$ - &  $\text{MnO}$ - $\text{Nb}_2\text{O}_5$ -type and  $\text{MnO}$ - $\text{Nb}_2\text{O}_5$ -type inclusions, which could be expressed as Equations (1)–(3).

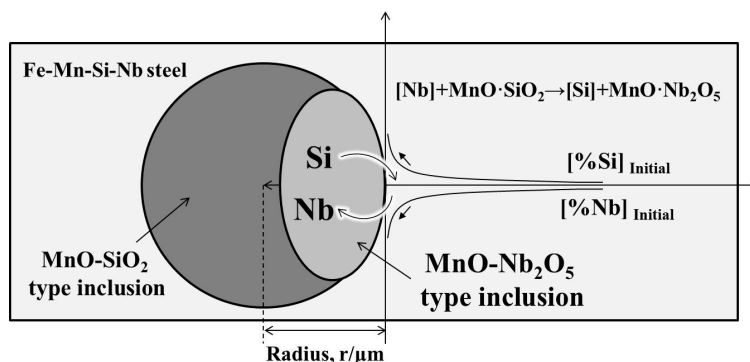
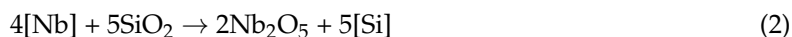


**Figure 7.** Schematic of interface reaction mechanism between the Fe-Mn-Si-Nb alloy and  $\text{MnO}$ - $\text{SiO}_2$ -type inclusions.

The transformation from original  $\text{MnO}$ - $\text{SiO}_2$ -type to  $\text{MnO}$ - $\text{SiO}_2$ - &  $\text{MnO}$ - $\text{Nb}_2\text{O}_5$ -type and  $\text{MnO}$ - $\text{Nb}_2\text{O}_5$ -type is beneficial to reducing cracks in alloys during rolling due to the decrease in melting point and hardness [14]. In addition, as long as the mechanism of the interface reaction between the alloy and M-S-type inclusion is clarified, it is probable to control and optimize the physiochemical characteristics of the inclusions in the niobium alloy and obtain fine and dispersed non-metallic inclusions by an appropriate heat treatment processes.

#### 4.2. The Equilibrium Relation between the Alloy and the Oxide Inclusions

The chemical compositions of stable oxide inclusions in the alloy samples containing different concentrations of Mn, Si, and Nb, at 1873 K and 1473 K, are estimated. This estimation is performed using Wagner's model for a multicomponent solution system [15], the regular solution model [16], and correlative thermodynamic data shown in Table 3. Oxygen activities for the formation of  $\text{SiO}_2$ , and  $\text{MnO}$ - $\text{SiO}_2$ -type and  $\text{MnO}$ - $\text{Nb}_2\text{O}_5$ -type inclusions, are then compared, based on the assumption that

the most stable oxide inclusion is obtained at the lowest oxygen activity. In addition, it was observed that a large proportion of final stable oxide inclusions were approximate  $\text{MnO}\cdot\text{SiO}_2$  and  $\text{MnO}\cdot\text{Nb}_2\text{O}_5$  formation based on EPMA analysis. Therefore, equilibrium calculation was conducted by assuming the formation of pure  $\text{MnO}\cdot\text{SiO}_2$  and  $\text{MnO}\cdot\text{Nb}_2\text{O}_5$ . The interaction coefficient of each element in the alloys, which is represented as  $e_i^j$ , is listed in Table 4. These thermodynamic data (see Tables 3 and 4 [17]) are also employed for approximate calculations of the equilibrium conditions between the alloy sample and oxide inclusion at 1473 K, although these data are inadequate for extrapolation to this temperature. The activities of MnO and  $\text{SiO}_2$  in manganese silicate were also estimated and verified using the experimental results from [17]. At 1473 K,  $\text{MnO}\cdot\text{SiO}_2$  and  $\text{MnO}\cdot\text{Nb}_2\text{O}_5$  exist in the solid state, and their activities are assumed to be unity.

**Table 3.** Basic thermodynamic data for the equilibrium calculation.

No.	Reaction	$\Delta G^\ominus$ (J/mol)	Reference
1	$\text{Nb(s)} = [\text{Nb}]$	$-134,260 + 33.05T$	[18]
2	$4\text{Nb(s)} + 5\text{O}_2(\text{g}) = 2\text{Nb}_2\text{O}_5(\text{s})$	$-3,770,150 + 834.95T$	[19]
3	$\text{Mn(l)} + 1/2\text{O}_2(\text{g}) = \text{MnO(s)}$	$-399,000 + 82.4T$	[19]
4	$\text{O}_2(\text{g}) = [\text{O}]$	$-234,304 - 5.78T$	[20]
5	$\text{Mn(l)} = [\text{Mn}]$	$4083.6 - 38.16T$	[20]
6	$[\text{Si}] + 2[\text{O}] = \text{SiO}_2(\text{s})$	$-576,440 + 218.2T$	[21]
7	$\text{MnO(s)} + \text{SiO}_2(\text{s}) = \text{MnSiO}_3(\text{s})$	$-27,960 + 2.42T$	[21]
8	$\text{MnO(s)} + \text{Nb}_2\text{O}_5(\text{s}) = \text{MnNb}_2\text{O}_6(\text{s})$	$86,940 - 49.6T$	[22]

Note:  $T$ —Temperature, K.

**Table 4.** Interaction coefficient of each element in the Fe-Mn-Si-Nb alloy ( $e_i^j$ ).

$j \backslash i$	Mn	Si	Nb	O
Mn	0	$-1838/T + 0.964$	$413/T - 0.217$	$-0.083$
Si	$-0.0146$	0.0103	0	$-0.119$
Nb	0.0093	$-0.01$	0	$-19,970/T + 9.950$
O	$-0.021$	$-0.066$	$-3440/T + 1.717$	$-1750/T + 0.76$

Note:  $T$ —Temperature, K.

The equilibrium oxygen activities of stable oxide inclusions in alloy samples with different Nb and Si concentrations at 1873 K and 1473 K are shown in Figures 8–10. At both temperatures,  $\text{MnO}\cdot\text{Nb}_2\text{O}_5$ -type inclusion in 0.65 mass % Nb alloy (see Figure 8) are considerably more stable than the  $\text{MnO}\cdot\text{SiO}_2$ -type inclusion and the equilibrium oxygen activity associated with the  $\text{MnO}\cdot\text{Nb}_2\text{O}_5$ -type oxide inclusion is always lower than that of the  $\text{MnO}\cdot\text{SiO}_2$ -type inclusion, indicating that  $\text{MnO}\cdot\text{Nb}_2\text{O}_5$  forms prior to  $\text{MnO}\cdot\text{SiO}_2$ . At 1873 K, as the Nb content in the alloy decreased to 0.15 mass %, some  $\text{MnO}\cdot\text{SiO}_2$ -type and  $\text{MnO}\cdot\text{SiO}_2$ - &  $\text{MnO}\cdot\text{Nb}_2\text{O}_5$ -type oxide inclusions were generated. A critical Si concentration of 0.78 mass % for 0.15 mass % Nb alloy and 0.20 mass % for 0.05 mass % Nb alloy for the transformation between  $\text{MnO}\cdot\text{SiO}_2$ -type and  $\text{MnO}\cdot\text{Nb}_2\text{O}_5$ -type oxide inclusion was obtained according to the thermodynamic calculation, as shown in Figures 9a and 10a. At 1473 K (see Figures 9b and 10b), this transformation occurs at a critical Si content of 2.5 mass % for 0.15 mass % Nb alloy and 0.8 mass % for 0.05 mass % Nb alloy. This calculation results support that, at an Si content of 0.4 mass % and an Nb content of 0.65 mass % (Sample 2), the stable  $\text{MnO}\cdot\text{Nb}_2\text{O}_5$ -type oxide inclusion is retained during heat treatment at 1473 K, and the transformation from  $\text{MnO}\cdot\text{SiO}_2$ -type to  $\text{MnO}\cdot\text{Nb}_2\text{O}_5$ -type oxide inclusion in Alloy Samples 4 and 8 was promoted after heating. These calculation results agreed, in general, with the experimental results and revealed the mechanism of interface reaction between the Fe-Mn-Si-Nb alloy and  $\text{MnO}\cdot\text{SiO}_2$  oxide inclusion. More importantly, these results contribute to the prediction of stable oxide formation in alloy (before and after heat treatment), based on the Si, Mn, and Nb concentrations of the alloy.

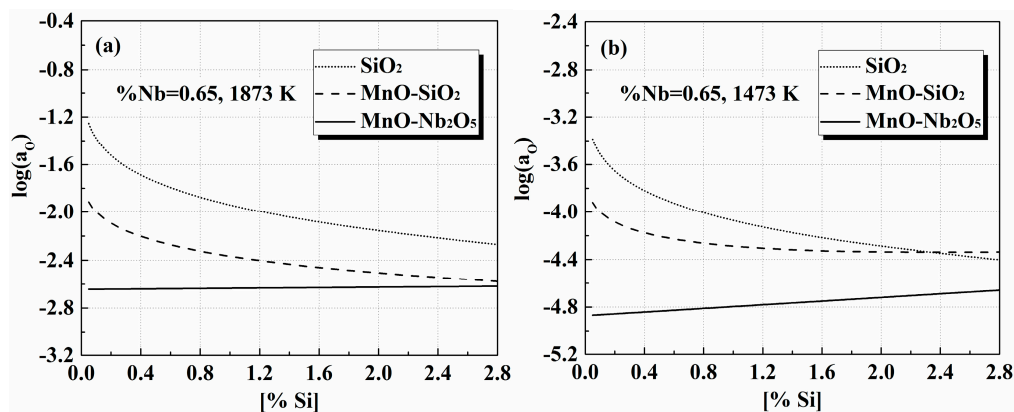


**Figure 8.** Equilibrium oxygen activities of stable oxide inclusions calculated at 1873 K (a) and 1473 K (b) corresponding to the alloy with 0.65 mass % Nb.

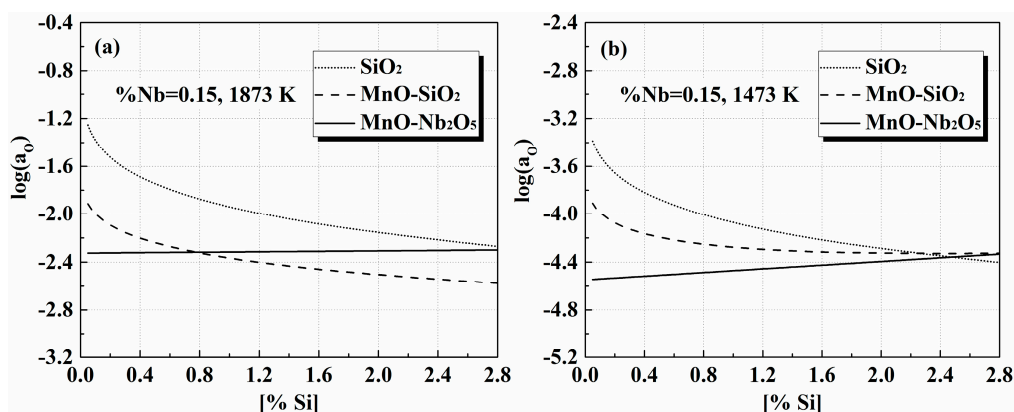


**Figure 9.** Equilibrium oxygen activities of stable oxide inclusions calculated at 1873 K (a) and 1473 K (b) corresponding to the alloy with 0.15 mass % Nb.

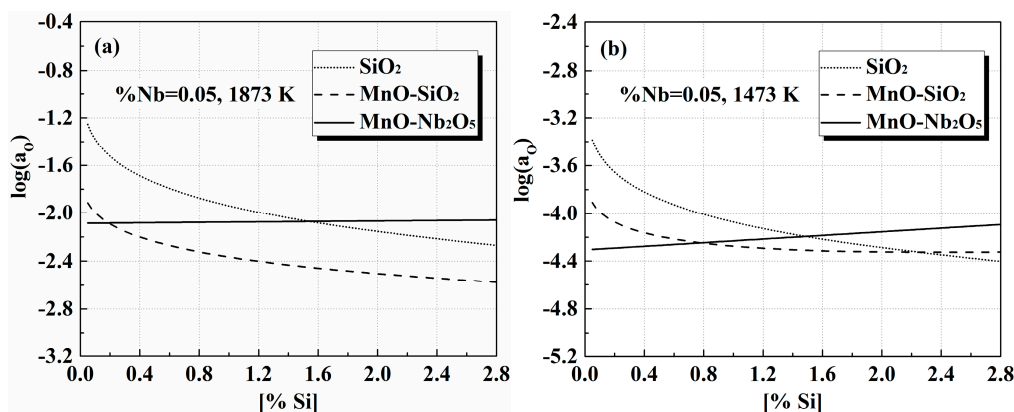


**Figure 10.** Equilibrium oxygen activities of stable oxide inclusions calculated at 1873 K (a) and 1473 K (b) corresponding to the alloy with 0.05 mass % Nb.

## 5. Conclusions

During the heating at 1473 K, the concentrations of Nb and Si in the alloys are critical for controlling the changing behavior of oxide inclusions. Stable oxide inclusions transformed from  $\text{MnO-SiO}_2$ -type to  $\text{MnO-Nb}_2\text{O}_5$ -type or  $\text{MnO-SiO}_2$ - &  $\text{MnO-Nb}_2\text{O}_5$ -type at low concentrations of Si and high concentration of Nb. It was indicated that an interface chemical reaction occurred between

the Fe-Mn-Si-Nb alloy matrix and the MnO-SiO<sub>2</sub>-type oxide inclusion. Estimation on the stable oxide inclusions in the alloys with different Nb concentrations by thermodynamic calculation at 1873 K and 1473 K basically matched the experimental results, thereby confirming the mechanism of the interface reaction. More significantly, the calculation results contribute to the prediction of heating-induced formation of a stable oxide, depending on the concentrations of Si, Mn, and Nb in the alloys.

**Acknowledgments:** This work was supported by the National Natural Science Foundation of China (Nos. 51604201 and 51574020) and the China Postdoctoral Science Foundation (No. 2016M602377).

**Author Contributions:** Chengsong Liu and Xiaoqin Liu conceived and designed the experiments; Chengsong Liu, Xiaoqin Liu and Fei Ye performed the experiments; Chengsong Liu, Xiaoqin Liu, Shufeng Yang, and Hongwei Ni analyzed the data; Jingshe Li and Hongwei Ni contributed reagents/materials/analysis tools; Chengsong Liu wrote the paper.

**Conflicts of Interest:** The authors declare no conflict of interest. The funding sponsors had no role in the design of the study; in the collection, analyses, or interpretation of data; in the writing of the manuscript; or in the decision to publish the results.

## References

1. Li, Y.; Wan, X.; Cheng, L.; Wu, K. Effect of oxides on nucleation of ferrite: First principle modelling and experimental approach. *Mater. Sci. Technol.* **2016**, *32*, 88–93. [[CrossRef](#)]
2. Yuan, Q.; Xu, G.; Zhou, M.; He, B.; Hu, H. The effect of p on the microstructure and melting temperature of Fe<sub>2</sub>SiO<sub>4</sub> in silicon-containing steels investigated by in situ observation. *Metals* **2017**, *7*, 37. [[CrossRef](#)]
3. Wakoh, M. Control of the size and the composition of oxide inclusions for oxides metallurgy. *Tetsu-to-Hagane* **2009**, *95*, 713–720.
4. Gao, X.; Yang, S.; Li, J.; Yang, Y.; Chattopadhyay, K.; Mclean, A. Effects of MgO nanoparticle additions on the structure and mechanical properties of continuously cast steel billets. *Metall. Mater. Trans. A* **2016**, *47B*, 461–470. [[CrossRef](#)]
5. Shibata, H.; Kimura, K.; Tanaka, T.; Kitamura, S. Mechanism of change in chemical composition of oxide inclusions in Fe-Cr Alloys deoxidized with Mn and Si by heat treatment at 1473 K. *ISIJ Int.* **2011**, *51*, 1944–1950. [[CrossRef](#)]
6. Choi, W.; Matsuura, H.; Tsukihashi, F. Changing behavior of non-metallic inclusions in solid iron deoxidized by Al-Ti addition during heating at 1473 K. *ISIJ Int.* **2011**, *51*, 1951–1956. [[CrossRef](#)]
7. Shao, X.; Wang, X.; Jiang, M.; Wang, W.; Huang, F. Effect of heat treatment conditions on shape control of large-sized elongated MnS inclusions in resulfurized free-cutting steels. *ISIJ Int.* **2011**, *51*, 1995–2001. [[CrossRef](#)]
8. Liu, C.; Yang, S.; Li, J.; Ni, H.; Zhang, X. Solid-state reaction between Fe-Al-Ca alloy and Al<sub>2</sub>O<sub>3</sub>-CaO-FeO oxide during heat treatment at 1473 K (1200 °C). *Metall. Mater. Trans. B* **2017**, *48B*, 1348–1357. [[CrossRef](#)]
9. Liu, C.; Ni, H.; Yang, S.; Li, J.; Ye, F. Interfacial reaction mechanism between multi-component oxides and solid alloys deoxidised by Mn and Si during heat treatment. *Ironmak. Steelmak.* **2017**, *44*. [[CrossRef](#)]
10. Koldaev, A.; D'yakonov, D.; Zaitsev, A.; Arutyunyan, N. Kinetics of the formation of nanosize niobium carbonitride precipitates in low-alloy structural steels. *Metallurgist* **2017**, *60*, 1032–1037. [[CrossRef](#)]
11. Liu, S.; Challa, V.; Natarajan, V.; Misra, R.; Sidorenko, D.; Mulholland, M.; Manohar, M.; Hartmann, J. Significant influence of carbon and niobium on the precipitation behavior and microstructural evolution and their consequent impact on mechanical properties in microalloyed steels. *Mater. Sci. Eng. A Struct.* **2017**, *683*, 70–82. [[CrossRef](#)]
12. Kang, Y.; Jung, I. Thermodynamic Modelling of pyrometallurgical oxide systems containing Mn oxides. In Proceedings of the VIII International Conference on Molten Slags, Fluxes and Salts, Santiago, Chile, 18–21 January 2009; Sánchez, M., Parra, P., Riveros, G., Díaz, C., Eds.; Quebecor World: Montreal, Chile, 2009.
13. Zhao, L. XPS study of the thermal stability of niobium surface oxides. *Acta Phys. Chim. Sin.* **1988**, *4*, 558–560.
14. Han, H.; Lin, Q.; Wei, S. Binary system 4MnO-Nb<sub>2</sub>O<sub>5</sub>-SiO<sub>2</sub>—One of the binary sections in the ternary system MnO-Nb<sub>2</sub>O<sub>5</sub>-SiO<sub>2</sub>. *Chin. J. Met. Sci. Technol.* **1990**, *6*, 136–138.
15. Takada, J.; Yamamoto, S.; Kikuchi, S.; Adachi, M. Determination of diffusion coefficient of oxygen in  $\gamma$ -iron from measurements of internal oxidation in Fe-Al alloys. *Metall. Trans. A* **1986**, *17A*, 221–229. [[CrossRef](#)]

16. Ban-Ya, S. Mathematical expression of slag-metal reactions in steelmaking process by quadratic formalism based on the regular solution model. *ISIJ Int.* **1993**, *33*, 2–11. [[CrossRef](#)]
17. Hino, M.; Ito, K. *Thermodynamic Data for Steelmaking*, 1st ed.; Tohoku University Press: Sendai, Japan, 2010; pp. 167–170.
18. Zhang, S.; Wei, S.; Wang, R.; Li, L. Electrochemical study of activity of Nb<sub>2</sub>O<sub>5</sub> and MnO in Nb<sub>2</sub>O<sub>5</sub>-MnO-SiO<sub>2</sub> system. *Acta Metall. Sin.* **1990**, *26*, B11–B15.
19. Ban-Ya, S.; Tatsuhiko, E.; Mitsuo, S. *Physical Chemistry of Metals*, 1st ed.; Maruzen Press: Tokyo, Japan, 1996; pp. 204–205.
20. Turkdogan, E.T. *Physical Chemistry of High Temperature Technology*, 1st ed.; Academic Press: New York, NY, USA, 1980; p. 81.
21. Shibata, H.; Tanaka, T.; Kimura, K.; Kitamura, S. Composition change in oxide inclusions of stainless steel by heat treatment. *Ironmak. Steelmak.* **2010**, *37*, 522–528. [[CrossRef](#)]
22. Han, H.; Lin, Q.; Wei, S. Binary system MnO-Nb<sub>2</sub>O<sub>5</sub>. *Chin. J. Met. Sci. Technol.* **1990**, *6*, 98–102.



© 2017 by the authors. Licensee MDPI, Basel, Switzerland. This article is an open access article distributed under the terms and conditions of the Creative Commons Attribution (CC BY) license (<http://creativecommons.org/licenses/by/4.0/>).